Curing of urethane dimetracrylate composites: A glass transition study

Jean-François Nguyen [a,b], Benjamin Pomes [a,b,d], Michaël Sadoun [c], Emmanuel Richaud [d,*]

[a] UFR d'Odontologie Université Paris Diderot, Paris, France
[b] PSL Research University, Chimie ParisTech CNRS, Institut de Recherche de Chimie Paris, Paris, France
[c] MaJEB sprl, Liège, Belgium
[d] Arts et Métiers ParisTech, Laboratoire de Procédés et Ingénierie en Mécanique et Matériaux (PIMM), CNRS, CNAM, UMR, 8006, France

Keywords:
Poly(urethane dimethacrylate)
Composites
Curing degree
Polymerization pressure
Glass transition

A B S T R A C T

Urethane dimethacrylate thermosets (UDMA) and their composites (PICN) were cured under varying polymerization pressures (1–3500 bars) and the resulting materials were characterized mainly by dynamic mechanical analysis (DMA) to measure their glass transition. In the case of PICN, glass transition displays an optimum in the middle pressure range (1000–2000 bars), which is linked to the conversion degree of polymerization process as measured by near infrared (NIR) spectrometry whereas it displays hyperbolic increase for UDMA networks. The results were discussed using classical theories used for describing the glass transition of networks. For samples post-cured at 160 °C during 1 h, the glass transition of undercured samples (1–1000 bars and P > 3000 bars) is shown to increase in link with possible post-curing. Reversely, the T_g of the most cured samples (polymerization pressure about 2000 bars) decreases which was attributed to the possible thermal decomposition. The glass transition temperature is here tentatively proposed a marker of the network architecture for samples varying by their processing (curing, post-curing) conditions and possibly their degradation level.

1. Introduction

Urethane Dimethacrylate (UDMA) based polymers are increasingly used for dental restorations in particular as matrices of Polymer Infiltrated Composite Networks (PICN) composite blocks used in Computer-aided design/computer-aided manufacturing (CAD-CAM) systems. Such materials are currently in full development making possible to simplify the manufacturing steps [1] and to use materials that are difficult to be processed by artisanal methods [2].

In such composites, one of the main requirements is to reach relatively high monomer conversion degrees (DC) so as to improve the mechanical properties and limit the release in oral environment of unreacted or monoreacted monomers that could be liberated by hydrolysis reactions [3,4]. However, it remains quite difficult to reach 100% curing degree [5,6]. Since dental practitioners such as prosthodontists expect good mechanical and physical properties, lasting quality and ageing resistance for their patients' dental restorations, the control of network architecture is a crucial issue for manufacturers which must carefully check it.

In the range of conversion degrees of interest (70–100%), the polymer networks are in their glassy state (at body temperature). In such conditions, it is known that elastic modulus mainly depends on the Cohesive Density Energy [7]. Both values only slightly change in the high conversion degrees range [8,9] (in particular in networks without any sub-glassy relaxation i.e. where there is almost no motion of short segments). Another study reports changes of hardness with conversion degrees in dental composites [10] but the investigated conversion degree range is lower than for CAD-CAM purpose (about 65% versus more than 90%). Moreover, hardness is no, to our knowledge, described theoretical structure-properties relationships. Above glass transition, the rubbery modulus is known to linearly increase with the conversion degree [11] (linked to the crosslink density). However, estimations can be flawed because of chemical changes occurring at such elevated temperatures. Moreover, dental composites usually are highly filled [12]. Consequently, their elastic moduli both in glassy and rubbery states depend in great part of fillers content and on filler-matrix interfacial effects as well which complicates the estimation of the real state of the matrix.

In other words, a fine description of the network architecture still is needed. This tracker must strongly vary in the range of conversion degrees where mechanical properties of acrylate composites are in line with practitioners' requirements, so as to be later used for describing the

* Corresponding author.
E-mail address: emmanuel.richaud@ensam.eu (E. Richaud).

effect of water or thermal ageing of those networks.

We will hence discuss on the reliability of glass transition measurements in the case of UDMA networks and their composites considered here respectively as model and real systems. The glass transition measurements will be discussed using structure-properties relationships to validate the relation in the case of acrylate networks.

2. Experimental

2.1. Materials

A mixture of UDMA (UDMA; M = 470.56 g mol^{-1}; CAS 41137-60-4 supplied by Esstech, Germany) and benzoyl peroxide (BPO supplied by Sigma Aldrich, Steinheim, Germany) was used to produce the UDMA polymers and PICN blocks samples in this study. Weight ratios were 99.5:0.5%. Fillers for PICN composite were VITA Mark II glass ceramic powder (VITA Zahnfabrik, Germany) with a characteristic size 5.13 µm as D50 (i.e. 50% particles are lower than 5.13 µm).

UDMA structure before and after polymerization are given in Scheme 1 (NB: the pure thermoset will be denoted UDMA in the following).

2.2. Sample manufacturing

A slip was obtained by mixing in a planetary mixer (Thinky ARE-250, Thinky Corporation, Tokyo, Japan) the glass-ceramic powder with a volume fraction of 56% and water. This was then poured into a plaster mold and left to dry overnight at room temperature to agglomerate the grains. After demolding, the blocks obtained were dehydrated at 160 °C for 2 h in an oven and then sintered at 800 °C for 2 h. The sintered blocks were then silanated with pre-hydrolyzed methacryl-oxypropyl-tri-oxy-silane (Sigma Aldrich, Saint-Louis, USA) and then heated at 140 °C for 6 h. Infiltration of the mixture of UDMA (99.5% by weight) and benzoyl peroxide (0.5% by weight) of the sintered blocks was carried out under vacuum.

UDMA polymers and PICN blocks were polymerized for 4 h at 90 °C at a pressure ranging from 1 bar to 3500 bars in a self-built autoclave with a range of 500 bars. Some samples (denoted by PC) were post-cured at 160 °C for 1 h in an oven (Memmert, Schwabach, Germany). The manufacturing details are specified in Table 1.

2.3. Characterization

2.3.1. Differential scanning calorimetry

Samples curing were characterized by Q1000 DSC (TA Instruments) driven by QSeries Explorer. Uncured reactive mixtures were heated in sealed hermetic standard pans from − 75 to 225 °C at a 40 °C min^{-1} rate. This high heating rate was chosen to better observe T_g. DSC cell was purged by a 50 ml min^{-1} nitrogen flow. Experiments were exploited using TA Universal Analysis software. Apparatus was calibrated with indium (for temperature) and sapphire (for heat capacity) standards prior to analyses. DSC analyses were performed to measure T_g of uncured monomer (T_{g0}) and fully cured mixtures (T_{g100}), and estimate the corresponding heat capacity jumps ΔC_{P0} and ΔC_{P100}.

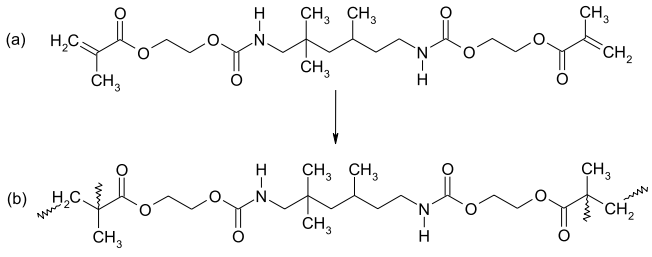

Scheme 1. UDMA monomer before (a) and after (b) polymerization.

2.3.2. Dynamical mechanical analysis

DMA were performed according to Refs. [13,14]. Experiments were conducted on eight 4 mm × 20 mm x 1 mm samples using a DMA 7/DX apparatus (PerkinElmer, Waltham, MA, USA) in 3 points bending mode with 15 mm distance, at a 1 Hz frequency. Static and dynamic load were taken respectively equal to 2.5 N and 2 N for composite and 0.3 N and 0.2 N for UDMA (corresponding to maximal amplitude about 18–28 µm for PICN and 30 µm for UDMA). Samples were heated from 30 °C to 180 °C with 2 °C min^{-1} heating ramp. Indium and steel standards were used to calibrate respectively thermocouple and stiffness. Other calibrations were performed according to supplier data. Glass transition temperature (T_g) was determined as the maximal temperature of tan δ peak. Elastic and loss moduli were not exploited here.

2.3.3. Near InfraRed spectroscopy

Ten 19 mm × 12 mm × 1 mm samples were cut using an isomet (Buehler, Lake Bluff, Il, USA) and polished using SiC under water. Curing degree (DC) was measured using a FTIR Nicolet IS-10 (Thermo Scientific, Madison, WI, USA) in Near InfraRed transmission using a NIR 714–016300 source (Thermo Scientific, Madison, WI, USA). Spectra were obtained by averaging 384 scan with a 2 cm^{-1} resolution. DC was determined from the =CH absorption peak at 6164 cm^{-1} using the following equation [15,16]:

$$DC(\%) = \left(1 - \frac{P}{M}\right) \times 100$$

P and M being respectively the areas measured for the PICN network and a monomer-filler blend. Results were previously shown to be consistent with those based on MID-IR measurements of C=C absorption peak at 1637 cm^{-1} [15,16].

3. Results

3.1. In situ curing by DSC

Thermograms for in situ curing are given in Fig. 1. They display:

- for the first ramp: the glass transition of the uncured monomer (T_{g0}) at about −30 °C with the corresponding heat capacity jump (ΔC_{P0}) and the curing exotherm with an onset a about 90 °C.
- for the second heating ramp, the glass transition of the cured network ($T_{g\infty}$) is observed from the maximal derivative between slopes at 25 and 225 °C (as schematized in Fig. 1), with the corresponding heat capacity jump (ΔC_{P100}).

The results are gathered in Table 2. They will be used later as input for the Pascault Di Benedetto law.

3.2. Glass transition of UDMA networks and PICN composites

The glass transition measured by DMA of UDMA networks and PICN composites polymerized under several pressures are given in Fig. 2 with a comparison for cured and post-cured materials. It calls for the following comments:

- For the cured UDMA networks, the glass transition plateaus for polymerization pressures higher than 1000 bars with a maximal glass transition close to 135 °C. High pressure effects on polymerization have been earlier described [17–19]. At first, increasing pressure brings the monomers closer, thus increasing polymerization kinetics [20]. Reversely, when pressure gets too high, mobility decreases together with polymerization rate. A supplementary effect is due to the presence of fillers absorbing a part of polymerization heat release which explains why the glass transition decrease in the case of PICN cured under

Table 1
Details of materials.

Pressure Polymerization (bar)	Materials	Matrix	Initiator	Filler	Polymerization	Post-Polymerization parameters
1-500-1000-1500-2000-2500-3000-3500	PICN	UDMA	0.5% PBO	VITA Mark II (73.8% by weight)	90 °C 4 h	None 160 °C 1 h
	UDMA polymer	UDMA	0.5% PBO	–	90 °C 4 h	none

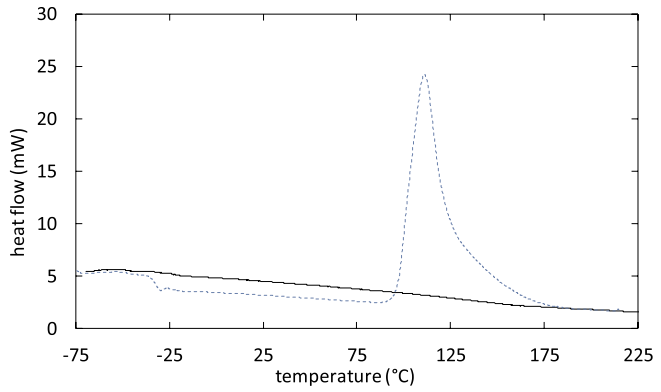

Fig. 1. DSC thermogram of uncured (dashed line) and fully cured (full fine) UDMA.

Table 2
Glass transition (T_g) and heat capacity jump at glass transition (ΔC_p) for monomer (subscript 0) and fully cured (subscript 100) polymer (average for n = 4 tests) measured by DSC.

T_{g0}	ΔC_{P0}	T_{g100}	ΔC_{P100}	$\lambda = \Delta C_{P100}/\Delta C_{P0}$	$(T_{g100} - T_{g0})/\lambda$
−30.7	0.585	137.9	0.470	0.806	209.4

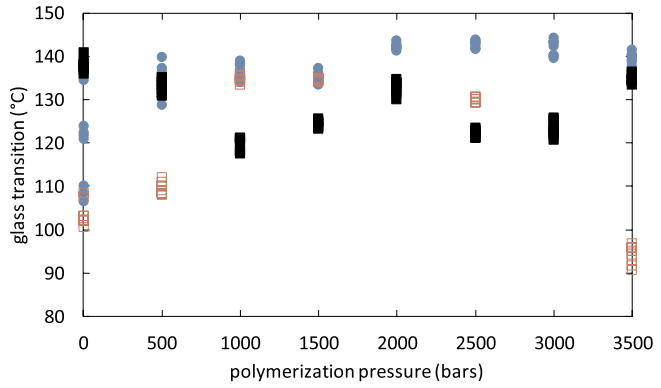

Fig. 2. Glass transition of networks (from DMA measurements) cured under several external polymerization pressures for UDMA networks without post-curing (●), UDMA based composites (□) and with (■) post-curing.

enhanced pressures [21].

- In the case of post-cured composites, a "reverse" effect is observed: "poorly" cured PICN networks (for example for polymerization pressures equal to 1 and 3500 bars) are observed to display a significant increase in glass transition. For PICN with an initially high T_g before post-curing (for example 1000 bars), a decrease is observed.

To better understand those results, the glass transition values were plotted versus the curing degree (i.e. the conversion degree of double bonds). It can hence be seen that there is a linear correlation for non post-cured sample, but not for the post-cured samples for which the main trend is a T_g decrease. According to Fig. 3, the maximal T_g would be 421 K for UDMA and 417 K for its composite (which is consistent with T_{g100} suggested from the curing study by DSC – see Table 2).

4. Discussion

The aims of this section are to discuss:

- the maximal glass transition value corresponding to the fully cured networks (Fig. 3),
- the changes of glass transition in the observed for the high conversion degrees (Fig. 3),
- the (unexpected) origin of the post-curing (Fig. 2).

4.1. On the maximal value of glass transition for fully cured networks

Based on entropic considerations, DiMarzio [22] proposed a relation in which the glass transition temperature of a fully cured network is calculated from the crosslink density (x):

$$T_g = \frac{T_{gl}}{1 - (K_{DM} F x)} \quad (1)$$

where:

- T_{gl} is the glass transition temperature of the linear polymer (i.e. for example the uncured elastomer in the case of vulcanized elastomers),
- K_{DM} is an universal constant linked to the functionality of crosslink nodes (for example close to 3 in the case of epoxy-diamine networks where crosslink nodes are nitrogen atoms brought by hardener),
- F is the flex parameter expressing the average molar mass per rotatable bonds,

Bellenger and Verdu [23] proposed later an additive method for predicting T_{gl} in the case of crosslinked networks from the structure of the constitutive repetitive unit (but where crosslink nodes are removed). In UDMA networks, this latter is made of:

- 2 short chains made of one methyl group (–CH_2–),
- one long chain containing the segment with two esters and two urethanes groups.

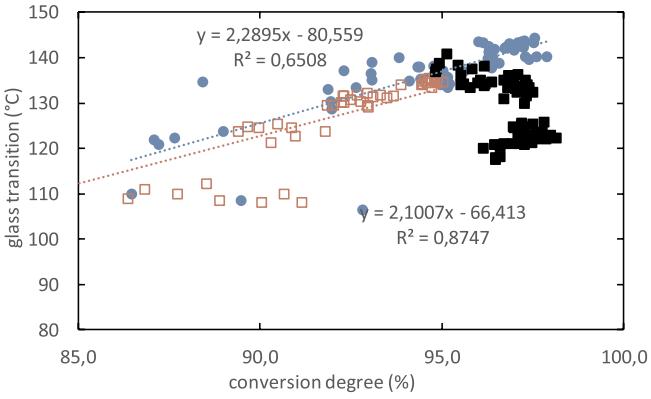

Fig. 3. Changes of glass transition versus conversion degree for UDMA networks without post-curing (●), UDMA based composites (□) and with (■) post-curing.

According to the method proposed in [23], T_{gl} can be given by:

$$T_{gl} = \frac{M_{UCR}^{*}}{\sum M_i \, T_{gli}^{-1}} \tag{2}$$

which gives in our case:

$$\frac{M}{T_{gl}} = 10 \times \left(\frac{M}{T_g}\right)_{>CH_2} + 2 \times \left(\frac{M}{T_g}\right)_{ester} + 2 \times \left(\frac{M}{T_g}\right)_{urethane} + \left(\frac{M}{T_g}\right)_{>C(CH_3)_2} + \left(\frac{M}{T_g}\right)_{>CH-CH_3} \tag{3}$$

The contributions for methylene and isopropyl groups are given in [23], contrarily to ester, urethane and ethyl (>C–CH_3) groups. Those latter were estimated from the glass transition of some well-chosen linear polymers (see Appendix A):

$$\frac{M}{T_{gl}} = 10 \times 0.06 + 2 \times 0.122 + 2 \times 0.1577 + 0.07586 + 0.0938 = 1.37386$$

So that:

$T_{gl} = 416/1.3738 = 313$ K

For the flex:

$$F = (F_1 + F_2 + F_3)/3 \tag{4}$$

F_1, F_2 and F_3 being the flex of each segment linked to a crosslink node, i.e. in our case:

- 2 methylene segments (M = 14 g mol^{-1}) with 1 flexible bond so that $F_1 = F_2 = 14$ g mol^{-1}
- 1 long segment made of the UDMA main chain (M = 388, 15 flexible bonds) so that $F_3 = 25.9$ g mol^{-1}

Finally:

$F = 18$ g mol^{-1}

Each UDMA gives 2 crosslink nodes so that, in a case of 100% cured network, x_{100} is given by:

$x_{100} = 2[UDMA] = 2/M_{UDMA} = 4.255$ mol kg^{-1}

T_{gl}, F and x_{100} values lead to $T_g = 403$ K consistently with T_{g100} values from Fig. 3 (less than 5% error).

4.2. On the effect of curing degree on glass transition

In this paragraph, we will compare the estimations coming from two models aimed at predicting T_g networks:

- The Pascault-DiBenedetto law, based on a mixture law of the entropy of the cured network and unreacted monomer [24,25],
- a modified DiMarzio law in which the crosslink density is calculated from the conversion degree.

Pascault-DiBenedetto proposed the following equation:

$$\frac{T_g - T_{g0}}{T_{g100} - T_g} = \frac{\lambda . DC}{1 - (1 - \lambda) . DC} \tag{5}$$

where T_{g0} and T_{g100} are the glass transition for monomer and fully cured polymer and $\lambda = \Delta C_{P\infty}/\Delta C_{P0}$ is the ratio of heat capacity jump at T_g. Eq. (5) can be derived as:

$$\frac{dT_g}{dDC} = (T_{g100} - T_{g0}) \cdot \frac{\lambda}{[1 - (1 - \lambda) . DC]^2} \tag{6}$$

In the high conversion domain ($x \to 1$), it can be written $x = 1 - \varepsilon$ with $\varepsilon \ll 1$ so that:

$$\frac{dT_g}{dDC} \underset{\varepsilon \to 0}{\approx} \frac{(T_{g100} - T_{g0})}{\lambda} \cdot \left(1 + 2 \cdot \frac{1 - \lambda}{\lambda} \cdot \varepsilon\right) \tag{7}$$

which can be approximated as:

$$\frac{dT_g}{dDC} \underset{\varepsilon \to 0}{\approx} \frac{(T_{g100} - T_{g0})}{\lambda} \tag{8}$$

According to data given in Table 2, the theoretical slope (210 K) is actually very close to experimental observations (Fig. 3) i.e. 210 K for the composite and 230 K for the UDMA network. In other words, our results are consistent with Pascault DiBenedetto law at least in the high conversion degrees range.

Let us now turn to the DiMarzio law which is here expressed as:

- For the fully cured network:

$$T_{g100} = \frac{T_{gl}}{1 - (K_{DM} F x_{100})} \tag{9}$$

- For the unfully cured network:

$$T_g = \frac{T_{gl}}{1 - (K_{DM} F x)} \tag{10}$$

Combining Eqs. (9) and (10) gives:

$$T_{g100} - T_g = \frac{T_{gl}}{1 - (K_{DM} F x_{100})} - \frac{T_{gl}}{1 - (K_{DM} F x)} \tag{11}$$

And:

$$T_{g100} - T_g = \frac{KFT_{gl} \, (x_{100} - x)}{(1 - K_{DM} F x_{100})(1 - K_{DM} F x)} \tag{12}$$

In the range of high conversion: $x \sim x_{100}$, so that:

$$T_{g100} - T_{g\sim} \frac{KFT_{gl} \, (x_{100} - x)}{(1 - K_{DM} F x_{100})^2} \tag{13}$$

In the case of chemically degraded trifunctional networks [26], a chain scission induces the loss of 3 elastically active chains. Assuming that uncured monomers having one unreacted double bond are equivalent to dangling chains coming from chain scissions, it gives:

$$n_{100} - n = 3[>C{=}{=}C<] \tag{14}$$

with:

$$[>C{=}{=}C<] = (1 - DC).[>C{=}{=}C<]_{100} = (1 - DC).2.[UDMA] \tag{15}$$

The number of elastically active chains is hence:

$$n_{100} - n = 6. \, (1 - DC).[UDMA] \tag{16}$$

So that, using:

$$n = (f/2).x \tag{17}$$

f is the network functionality which is here equal to 3. This gives:

$$x_{100} - x = 4. \, (1 - DC).[UDMA] \tag{18}$$

It gives:

$$T_g = T_{g\infty} - B + B.DC \tag{19}$$

with:

$$B = 4 \times [UDMA].K_{DM}.F.T_{g100}/(1\text{-}K_{DM}.F.2.[UDMA]) \tag{20}$$

So that:

$B = 230$ vs 220 K experimentally

In other words, prediction of T_g changes with DC from Eq. (20) are

consistent with experimental results. It is noteworthy that the structure-relationships proposed for ideal networks are here verified despite the relative complexity of UDMA networks and PICN matrices which are synthesized by radical processes where numerous structural "irregularities" head to head vs head to tail links, products resulting from transfer or dismutation process for example are expected.

4.3. On the post-curing effect

The last striking result to comment is the post-curing effect observed in PICN. For example, in the case of 1000 bars PICN, the T_g decreases by about 15 °C during post-curing whereas DC slightly increases (from about 95% to 97%). At first, it was checked that this is not due to physical ageing by structural relaxation which could provoke an apparent T_g increase [27] during the isothermal post-curing at 160 °C. Let us precise that glass transition seems much more influenced by curing degree [28] than by structural relaxation [29] at least in epoxy case. This was checked by DSC cycles (Fig. 4 - Appendix B) where the enthalpy overshoot characteristic of relaxation is not observed. The most reasonable explanation for us is the existence of chain scissions induced during the post-curing. Their concentration can be approximated from [26]:

$$n = n_{100} - 3s \tag{21}$$

Which gives:

$$s = \frac{T_{gl}}{2K_{DM}F} \times \left(\frac{1}{T_{gpost\ cured}} - \frac{1}{T_g}\right) \tag{22}$$

It can hence be seen that $s \sim 0.3\ mol\ kg^{-1}$ i.e. about 5% of initially present elastically active chains are cut. Interestingly, despite their reliability was recently addressed [30], elastic moduli values remain almost constant, as expected in highly filled composites where elastic moduli depends in great part of filler volume ratio. In other words, measurements of elastic modulus are not sensitive enough to detect the first stages of degradation contrarily to glass transition ones.

It remains to explain why this post-curing induced degradation is strong in some samples (typically those being well polymerized) whereas it is almost negligible for others (typically the less cured ones, e.g. those polymerized under 1 b and 3500 bars). Let us recall that crosslink bridges are formed:

- during propagation events (Scheme 2).
- during termination events (Scheme 3).

They can be destroyed by a "depolymerization" process. It is actually well known that, due to steric hindrance of the lateral substituents, the polymerization enthalpy of methyl methacrylate is reported to be lower than in many other polymers [31,32]. It results in a lower monomer-monomer bond enthalpy which explains why the thermal degradation of PMMA yields to the release of a high quantity of

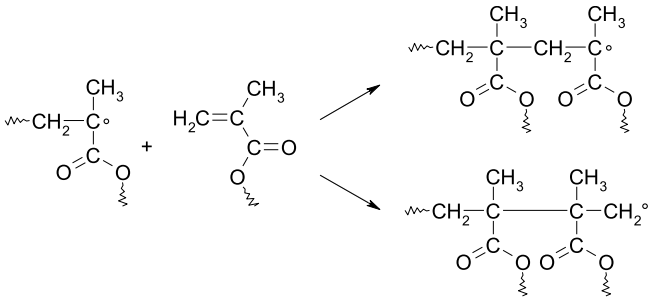

Scheme 2. Formation of crosslinked bridges by head to tail (up) and head to head (down) propagation reactions.

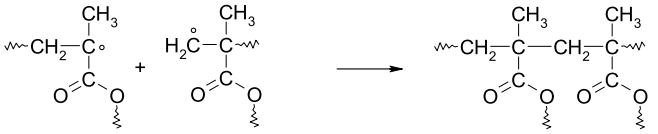

Scheme 3. Formation of crosslinked bridges by termination reactions.

monomer [33] accompanied by chain scissions [34]. The general mechanisms are well known and illustrated in Scheme 4 even if some peculiarities are expected in the case of UDMA networks since two chain scissions occurring on both extremities of UDMA monomer are needed to generate volatile. It is also clear that this mechanism is favored if samples are unfully polymerized.

The process is reported to start at relatively low temperature (125 °C [32] to 140 °C [35]). In other words, post-curing of UDMA networks and PICN is performed in the "narrow" region of TTT diagram comprised between devitrification and degradation [36]. The balance for crosslink formation is:

$$\frac{dx}{dt} = \gamma k_i [P^\circ]^2 + k_p [P^\circ][M] - k_i x \tag{23}$$

k_i being the rate constant for the decomposition reaction (possibly differing for head to head and HT head to tail isomers depicted in Scheme 2).

It can be assumed that the crosslinks formation is predominant for uncompletely crosslinked networks (justifying a T_g increase) whereas their destruction is predominant in fully crosslinked networks (consistently with the T_g decrease). This explanation is rather consistent with the gravimetric curves recorded using TGA under nitrogen (Fig. 5 - Appendix C) for UDMA samples: mass loss originates for chain scissions occurring at the vicinity of (uncured) dangling chains. Networks cured under 2000 bars display a lower mass loss level than networks cured under 1 and 1000 bars where the lower curing degree induces a higher mass loss level. As a prospect, modeling of the co-existence of polymerization and decomposition mechanisms remains an open task so as to establish the TTT diagram.

5. Conclusions

UDMA samples and their composites were cured at 90 °C under several polymerization pressures and post-cured at 160 °C. The resulting glass transition values were measured by DMA. Glass transition was shown to increase almost linearly for samples without post-curing with an optimum glass transition about 140 °C for 100% cured samples and a depletion coefficient about 2.2 °C per percent of curing degree. Both values were justified from two well-known theories: DiMarzio and Pascault DiBenedetto. The value of glass transition is thus a reliable indicator of the ageing effects in UDMA networks. In the case of UDMA based dental materials, in addition to the thermally induced reactions discussed in this paper, the T_g changes can either originate from structural relaxation [37] (with a T_g increase), or water diffusion (with a T_g decrease) [38], with a possible interplay between them [39], or chemical degradation involving the hydrolysis of urethane [40] or ester functions [41] leading to T_g decrease [26] and at very long term the total destruction of network (also named "degelation" [42]).

APPENDIX A

The PP amorphous phase is characterized by a glass transition temperature close to 0 °C [43–45].

$$M/T_g = (M/T_g)_{CH2} + (M/T_g)_{>CH-CH3} = 42/273 = 0.1538\ g\ mol^{-1}\ K^{-1}$$

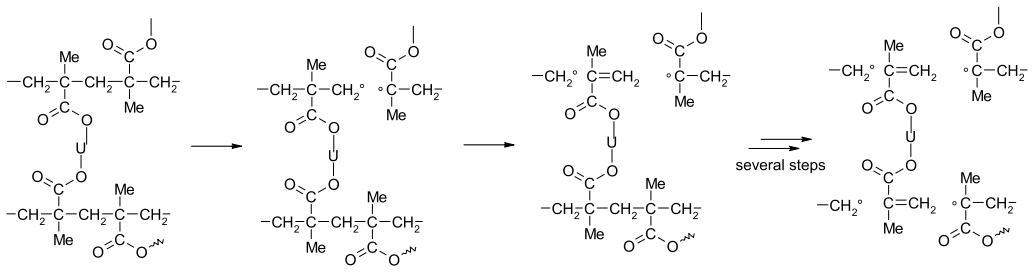

Scheme 4. Possible degradation mechanism with release of an UDMA group.

$(M/T_g)_{>CH-CH3} = 0.1538–0.06 = 0.0938\ g\ mol^{-1}\ K^{-1}$

The glass transition of PLA is reported to be about 333 K [46].

$M/T_g = (M/T_g)_{\ ester} + (M/T_g)_{>CH-CH3} = 72/333 = 0.216\ g\ mol^{-1}\ K^{-1}$

$(M/T_g)_{ester} = 0.216–0.0938 = 0.122\ g\ mol^{-1}\ K^{-1}$

In the case of diethylene glycol hexamehylene diisocyanate, T_g is about 280 K [47].

$M = 12 \times 12 + 5 \times 16 + 2 \times 14 + 22 = 274\ g\ mol^{-1}$

$M/T_g = 274/280 = 0.9785\ g\ mol^{-1}\ K^{-1}$

$M/T_g = 10 \times (M/T_g)_{CH2} + (M/T_g)_{>O} + 2 \times (M/Tg)_{urethane}$

$2*(M/T_g)_{urethane} = 0.5 \times (0.9785–10 \times 0.06–0.06306) = 0.1577\ g\ mol^{-1}\ K^{-1}$

APPENDIX B

DSC were performed according the following cycle:

- heating to 160 °C (40 °C min^{-1})
- isotherm at 160 °C (1 h) for simulating the post-curing.
- cooling at room temperature and heating at 200 °C (40 min^{-1}).

The most interesting results were obtained for samples cured under 1 bar. Analyses reveal:

- for first heating: T_g is relatively low (about 100 °C) in good agreement with DMA results. A slight exotherm might be observed just after the T_g in link with devitrification issue.
- for the second heating: the T_g is higher (here also in good agreement with DMA observations) but no overshoot (testimony of physical ageing by structural relaxation) is observed.

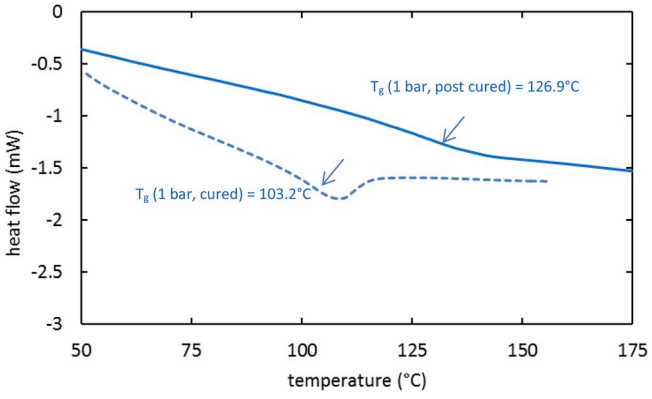

Fig. 4. DSC cycles for UDMA networks cured under 1 bar before (dashed line) and after post-curing (full line).

APPENDIX C

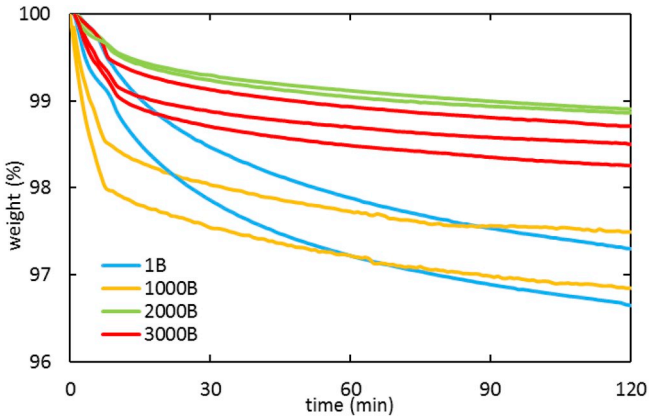

Fig. 5. TGA under nitrogen of UDMA networks cured under varying pressures for isothermal exposure at 160 °C under nitrogen.

References

[1] N.D. Ruse, M.J. Sadoun, Resin-composite blocks for dental CAD/CAM applications, J. Dent. Res. 93 (2014) 1232–1234.
[2] A.K. Mainjot, N.M. Dupont, J.C. Oudkerk, T.Y. Dewael, M.J. Sadoun, From artisanal to CAD-CAM blocks, J. Dent. Res. 95 (2016) 487–495.
[3] I.D. Sideridou, M.M. Karabela, Sorption of water, ethanol or ethanol/water solutions by light-cured dental dimethacrylate resins, Dent. Mater. 27 (10) (2011) 1003–1010.
[4] E. Putzeys, S. De Nys, S.M. Cokic, R. Corneliu Duca, J. Vanoirbeek, L. Godderis, B. Van Meerbeek, K.L. Van Landuyt, Long-term elution of monomers from resin-based dental composites, Dent. Mater. 35 (3) (2019) 477–485.
[5] J.W. Stansbury, S.H. Dickens, Network formation and compositional drift during photo-initiated copolymerization of dimethacrylate monomers, Polymer 42 (15) (2001) 6363–6369.
[6] I.M. Barszczewska-Rybarek, Characterization of urethane-dimethacrylate derivatives as alternative monomers for the restorative composite matrix, Dent. Mater. 30 (12) (2014) 1336–1344.
[7] J.-P. Pascault, H. Sautereau, J. Verdu, R.J.J. Williams, Thermosetting Polymers, Marcel Dekker, 2002. Chap 10. Basic Physical Properties of Networks.
[8] J.W. Stansbury, Dimethacrylate network formation and polymer property evolution as determined by the selection of monomers and curing conditions, Dent. Mater. 28 (2012) 13–22.
[9] B. Pomes, I. Derue, A. Lucas, J.-F. Nguyen, E. Richaud, Water ageing of urethane dimethacrylate networks, Polym. Degrad. Stab. 154 (2018) 195–202.
[10] A.C. Obici, M.A.C. Sinhoreti, E. Frollini, L.C. Sobrinho, S. Consani, Degree of conversion and knoop hardness of Z250 composite using different photo-activation methods, Polym. Test. 24 (2005) 814–818.
[11] J.E. Mark, A. Eisenberg, W.W. Graessley, L. Mandelkern, J.L. Koenig, Physical Properties of Polymers, ACS, Washington, DC, 1984, pp. 1–54. Chap. 1.
[12] S. Jager, R. Balthazard, M. Vincent, A. Dahoun, E. Mortier, Dynamic thermo-mechanical properties of various flowable resin composites, J. Clin. Exp. Dent. 8 (5) (2016) 534–539.
[13] A.C. Phan, P. Béhin, G. Stoclet, N.D. Ruse, J.-F. Nguyen, M. Sadoun, Optimum pressure for the high-pressure polymerization of urethane dimethacrylate, Dent. Mater. 31 (4) (2015) 406–412.
[14] P. Béhin, G. Stoclet, N.D. Ruse, M. Sadoun, Dynamic mechanical analysis of high pressure polymerized urethane dimethacrylate, Dent. Mater. 30 (2014) 728–734.
[15] J.W. Stansbury, S.H. Dickens, Determination of double bond conversion in dental resins by near infrared spectroscopy, Dent. Mater. 17 (2001) 71–79.
[16] J.L. Ferracane, T.J. Hilton, J.W. Stansbury, D.C. Watts, N. Silikas, N. Ilie, et al., Academy of Dental Materials guidance—resin composites: Part II—technique sensitivity (handling, polymerization, dimensional changes), Dent. Mater. 33 (2017) 1171–1791.
[17] E.W. Fawcett, R.O. Gibson, The influence of pressure on a number of organic reactions, in the liquid phase, J. Chem. Soc. (1934) 386–395.
[18] T. Arita, Y. Kayama, K. Ohno, Y. Tsujii, T. Fukuda, High-pressure atom transfer radical polymerization of methyl methacrylate for well-defined ultrahigh molecular-weight polymers, Polymer 49 (2008) 2426–2429.
[19] Y. Kojima, T. Matsuoka, H. Takahashi, Structure of poly (methyl methacrylate) synthesized under high pressure, J. Mater. Sci. Lett. 21 (2002) 473–475.
[20] V. Schettino, R. Bini, M. Ceppatelli, M. Citroni, Activation and control of chemical reactions at very high pressure, Phys. Scr. 78 (2008) 1–5.
[21] O. Nabinejad, D. Sujan, M.E. Rahman, I.J. Davies, Effect of filler load on the curing behavior and mechanical and thermal performance of wood flour filled thermoset composites, J. Clean. Prod. 164 (2017) 1145–1156.
[22] E.A. DiMarzio, On the second-order transition of a rubber, J. Res. Natl. Bur. Stand. Sect. A. Physic. Chem. 68 (1964) 611–617.
[23] V. Bellenger, J. Verdu, E. Morel, Effect of structure on glass transition temperature of amine crosslinked epoxies, J. Polym. Sci. B Polym. Phys. 25 (6) (1987) 1219–1234.
[24] J.P. Pascault, R.J.J. Williams, Glass transition temperature versus conversion relationships for thermosetting polymers, J. Polym. Sci. B Polym. Phys. 28 (1990) 85–98.
[25] J.P. Pascault, R.J.J. Williams, Relationships between glass transition temperature and conversion, Polym. Bull. 24 (1990) 115–121.
[26] E. Ernault, E. Richaud, B. Fayolle, Thermal-oxidation of epoxy/amine followed by glass transition temperature changes, Polym. Degrad. Stab. 138 (2017) 82–90.
[27] G.M. Odegard, A. Bandyopadhyay, Physical aging of epoxy polymers and their composites, J. Polym. Sci. B Polym. Phys. 49 (24) (2011) 695–1716.
[28] T.D. Chang, S.H. Carr, J.O. Brittain, Studies of epoxy resin systems: Part B: effect of crosslinking on the physical properties of an epoxy, Polym. Eng. Sci. 22 (1) (1982) 1213–1220.
[29] T.-D. Chang, J.O. Brittain, Studies of epoxy resin systems: Part C: effect of sub-tg, aging on the physical properties of a fully cured epoxy, Polym. Eng. Sci. 22 (1) (1982) 1221–1227.
[30] I.R. Henriques, L.A. Borges, M.F. Costa, B.G. Soares, D.A. Castello, Comparisons of complex modulus provided by different Dma, Polym. Test. 72 (2018) 394–406.
[31] D.E. Roberts, Heat of polymerization. A summary of published values and their relation to structure, J. Res. Natl. Bur. Stand. 44 (1950) 221–232.
[32] J.P. Chen, T. Kodaira, K. Isa, T. Sensa, Simultaneous TG-MS studies on polymers derived from monomers with a polar group, J. Mass Spectrom. Soc. Jpn. 49 (2) (2001) 41–50.
[33] W. Kaminsky, M. Predel, A. Sadiki, Feedstock recycling of polymers by pyrolysis in a fluidised bed, Polym. Degrad. Stab. 85 (2004) 1045–1050.
[34] G. Madras, V. Karmore, Continuous distribution kinetics for oxidative degradation of PMMA in solution, Polym. Degrad. Stab. 72 (2001) 537–541.
[35] T. Kashiwagi, A. Inaba, J.E. Brown, K. Hatada, T. Kitayama, E. Masuda, Effects of weak linkages on the thermal and oxidative degradation of poly(methyl methacrylates), Macromolecules 19 (1986) 2160–2168.
[36] S.L. Simon, J.K. Gillham, Reaction kinetics and TTT cure diagrams for off-stoichiometric ratios of a high-T, epoxy/amine system, J. Appl. Polym. Sci. 46 (1992) 1245–1270.
[37] G.M. Odegard, A. Bandyopadhyay, Physical aging of epoxy polymers and their composites, J. Polym. Sci. B Polym. Phys. 49 (2011) 1695–1716.
[38] B. De'Nève, M.E.R. Shanahan, Water absorption by an epoxy resin and its effect on the mechanical properties and infra-red spectra, Polymer 34 (24) (1993) 5099–5105.
[39] A. Le Guen-Geffroy, P.-Y. Le Gac, B. Habert, P. Davies, Physical ageing of epoxy in a wet environment: coupling between plasticization and physical ageing, Polym. Degrad. Stab. 168 (2019). Article 108947.
[40] P.Y. Le Gac, D. Choqueuse, D. Melot, Description and modeling of polyurethane hydrolysis used as thermal insulation in oil offshore conditions, Polym. Test. 32 (2013) 1588–1593.
[41] E. Richaud, P. Gilormini, M. Coquillat, J. Verdu, Crosslink density changes during the hydrolysis of tridimensional polyesters, Macromol. Theory Simul. 23 (2014) 320–330.
[42] P. Gilormini, E. Richaud, J. Verdu, A statistical theory of polymer network degradation, Polymer 55 (16) (2014) 3811–3817.
[43] M. Aguilar, J.F. Vega, B. Peña, J. Martínez-Salazar, Novel features of the rheological behaviour of metallocene catalysed atactic polypropylene, Polymer 44 (5) (2003) 1401–1407.
[44] J.H. Chen, F.C. Tsai, Y.H. Nien, P.H. Yeh, Isothermal crystallization of isotactic polypropylene blended with low molecular weight atactic polypropylene. Part I. Thermal properties and morphology development, Polymer 46 (15) (2005) 5680–5688.

[45] I. Schwarz, M. Stranz, M. Bonnet, J. Petermann, Changes of mechanical properties in cold-crystallized syndiotactic polypropylene during aging, Colloid Polym. Sci. 279 (5) (2001) 506–512.

[46] A.A. Marek, V. Verney, Photochemical reactivity of PLA at the vicinity of glass transition temperature. The photo-rheology method, Eur. Polym. J. 81 (2016) 239–246.

[47] https://polymerdatabase.com/polymers/hexamethylenediisocyanatediethyleneglycol.html.